ENHANCED POLYMER SOLAR CELLS EMBEDDED BY GOLD ENCAPSULATED SILVER PLASMONIC NANOPARTICLES

MUHEEB AHMAD MOUSA ALKHALAYFEH

UNIVERSITI SAINS MALAYSIA

2022

ENHANCED POLYMER SOLAR CELLS EMBEDDED BY GOLD ENCAPSULATED SILVER PLASMONIC NANOPARTICLES

by

MUHEEB AHMAD MOUSA ALKHALAYFEH

Thesis submitted in fulfilment of the requirements
for the degree of
Doctor of Philosophy

April 2022

ACKNOWLEDGEMENT

First of all, I would like to thank Almighty Allah for the many blessings He's bestowed upon me during my studies and in completing this thesis. May Allah's blessing goes to the final Prophets Muhammad peace be upon him, his family, and his companions.

I would like to express my sincere gratitude to my main supervisor, **Professor Dr. Azlan Abdul Aziz**, for his ongoing support during the past three years. I am so grateful for his motivation, enthusiasm, patience, immense knowledge, and expertise as well as his positive attitude.

I would like to sincerely appreciate my co-supervisor, **Dr. Mohd Zamir Pakhuruddin**, for his supportive manner and accurate knowledge. I am so thankful for his encouragement, and ongoing support during my work at Nor Lab.

I am eternally grateful to my loving family, including my devoted parents, beloved fiancée, brothers, and sisters, for their invaluable support and unending love. They have been so close to me, although we have been thousands of kilometers away for the past three years.

I am also thankful to all my friends for their whole-hearted help and valuable suggestions.

Muheeb Ahmad Alkhalayfeh

TABLE OF CONTENTS

LIST OF TABLES

Page

LIST OF FIGURES

Page

LIST OF SYMBOLS

Au@Ag	Silver-coated gold
CB	Conduction band
d	Particle size
D	Diffusion coefficient
E	Energy
E_{Fn}	Electron quasi-Fermi levels
E_{Fp}	Hole quasi-Fermi levels
eV	Electron volte
I	Flux of photons
I_0	Intensity
I_{max}	Maximum current
I_{sc}	Short circuit current
J_0	Saturation current density
J_{sc}	Short circuitcurrent density
K	Boltzmann constant
L_D	Length of diffusion
mA	Milliampere
°C	Degree Celsius

P_{max}	Maximum power
p-n	Positive-type and negative-type
q	Elementary charge
R_s	Series resistance
R_{sh}	Shunt resistance
VB	Valance band
V_{max}	Maximum voltage
V_{oc}	Open-circuit voltage
α	Absorption coefficient
λ	Wavelength
θ	Diffraction angle

LIST OF ABBREVIATIONS

AA	Ascorbic acid
AFM	Atomic force microscopy
Ag	Silver
Al	Aluminium
Au	Gold
BHJ	Bulk heterojunction
BT	Benzothiadiazole
CdTe	Cadmium telluride
$CH_3NH_3PbI_3$	Methylammonium lead iodide
CIGS	Copper indium gallium selenide
DSSCs	Dye-sensitized solar cells
EDX	Energy-dispersive X-ray spectroscopy
EM	Electromagnetic
FESEM	Field emission scanning electron microscopy
FF	Fill factor
$HAuCl_4$	Gold trichloride hydrochloride
HOMO	Highest occupied molecular orbital
HTL	Hole transport layer

IoT	Internet of Things
ITO	Indium tin oxide
J-V	Current density–voltage
LSPR	Localized surface plasmon resonance
LUMO	Lowest unoccupied molecular orbital
MIS	Metal-insulator-semiconductor
MNPs	Metallic nanoparticles
nm	Nanometre
NPs	Nanoparticles
P3HT	Poly(3-hexylthiophene)
$PC_{71}BM$	[6,6]-Phenyl C_{71}butyric acid methyl ester, mixture of isomers
PCE	Power conversion efficiency
PEDOT:PSS	Poly(3,4-4ethylenedioxythiophene):poly(styrenesulfonate)
PSCs	Polymer solar cells
PVP	polyvinylpyrrolidone
QDSSCs	Quantum dot-sensitized solar cells
SIS	Semiconductor-Insulator-Semiconductor
SPR	Surface Plasmonic Resonance
TEM	Transmission electron microscopy

UV-vis	Ultraviolet–visible spectroscopy
XRD	X-ray diffraction

SEL SURIA POLIMER DIPERTINGKATKAN DENGAN TERBENAM NANOPARTIKEL PLASMONIK EMAS DISELAPUT PERAK

ABSTRAK

Polimer semikonduktor organik berguna dalam beberapa aplikasi fotonik kerana sifat optik dan elektroniknya yang dapat disesuaikan dan kemudahan dalam pembuatannya. Walau bagaimanapun, oleh kerana panjang penyebaran eksiton pendek dan mobiliti pembawa yang rendah dalam sel suria polimer (PSC), kecekapan penukaran daya (PCE) mereka jauh lebih rendah daripada bahan bukan organik yang lain. Oleh itu, beberapa strategi telah dikembangkan untuk meningkatkan PCE PSC. Salah satu strategi adalah hasil kesan plasmonik, yang telah menunjukkan potensi aplikasi dalam PSC. Bentuk dan ukuran nanopartikel (NP) adalah faktor penting kerana ianya secara langsung mempengaruhi resonans plasmonik permukaan (SPR) dan penyerakan cahaya kejadian. Oleh itu, kajian ini memperkenalkan kesan plasmonik ke dalam PSC dengan memasukkan Au@Ag berbentuk durian untuk meningkatkan prestasinya. Au@Ag NP berbentuk durian plasmonik, yang boleh diletakkan di lapisan pengangkutan lubang (HTL) PSC, menyebarkan cahaya ke lapisan aktif, sehingga meningkatkan panjang jalur optik cahaya kejadian, menyebabkan penyerapan yang lebih tinggi dan pendek ketumpatan arus litar (J_{sc}) PSC. Sifat ukuran dan morfologi permukaan Au@Ag NP dianalisis menggunakan mikroskop elektron pengimbas pelepasan medan (FESEM) dan mikroskopi elektron transmisi (TEM). Topografi lapison PSC dengan dan tanpa Au@Ag NP disiasat menggunakan mikroskop daya atom (AFM). Spektroskopi UV-Vis dan analisis voltan ketumpatan arus (JV) digunakan untuk menyiasat prestasi elektrik PSC buatan. Bentuk yang dicadangkan Au@Ag NP menunjukkan kesan

jejari kecil ujung lonjakan. NP berbentuk durian pada prestasi PSC. Hasil kajian mendedahkan Jsc dan PCE sehingga 17 mA/cm^2 and 3.73%, masing-masing, yang menunjukkan kenaikan sebanyak 44.4% ketumpatan fotoarus litar pintas dan 49% kenaikan PCE berbanding sel rujukan (tanpa nanopartikel). Selain itu, nisbah isi yang berbeza PEDOT:PSS-pada-Au@Ag NP (8%, 10%, 12%, 14%, dan 16%) disediakan untuk mengoptimumkan keadaan sintesis untuk peningkatan kecekapan. Hasilnya, peranti dengan nisbah kelantangan 14% (PEDOT:PSS–pada–Au@Ag NP) menunjukkan penyerapan cahaya yang lebih baik dalam jarak gelombang yang luas dari 350 nm hingga 750 nm, di mana PCE diperbaiki dari 2.50 hingga 4.15%, yang merupakan peningkatan 66% berbanding dengan peranti tanpa NP. Di samping itu, Au @ Ag NP berbentuk durian yang tertanam di kedua lapisan aktif dan penyangga disiasat secara terperinci. Diperhatikan bahawa peranti plasmonik dengan struktur ITO / PEDOT:PSS + Au@Ag NP (14 %)/PTB7:$PC_{71}BM$ + Au@Ag NP (4%)/Al berfungsi lebih baik daripada yang lain. Oleh itu, kecekapan terbaik yang diperoleh dalam penyelidikan ini adalah 4.24%, yang mewakili peningkatan PCE sebanyak 69.6% berbanding dengan sel rujukan.

ENHANCED POLYMER SOLAR CELLS EMBEDDED BY GOLD ENCAPSULATED SILVER PLASMONIC NANOPARTICLES

ABSTRACT

Organic semiconducting polymers are useful in several photonic applications due to their tunable optical and electronic properties and ease of fabrication. However, due to the short exciton diffusion length and low carrier mobility in polymer solar cells (PSCs), their power conversion efficiency (PCE) is comparably lower than their inorganic counterparts. Therefore, several strategies have been developed to enhance the PCE of PSCs. One of the strategies is the plasmonic effect, which has shown potential applications in PSCs'. The shape and size of nanoparticles (NPs) are important factors since they directly affect surface plasmonic resonance (SPR) and the incident light's scattering. Therefore, this study introduces plasmonic effects into PSCs by incorporating Au@Ag durian-shaped NPs to improve their performance. The plasmonic durian-shaped Au@Ag NPs, which can be placed in the hole transport layer (HTL) of the PSC, scatter light into the active layer, thereby increasing the optical path length of the incident light, leading to higher absorption and short circuit current density (J_{sc}) of the PSCs. The size properties and surface morphology of the Au@Ag NPs were analyzed using field emission scanning electron microscopy (FESEM), transmission electron microscopy (TEM). The topography of the PSCs' layers with and without Au@Ag NPs was investigated using atomic force microscopy (AFM). UV–Vis spectroscopy and current density–voltage (J-V) analysis were used to investigate the electrical performance of the fabricated PSCs. The PCE and J_{sc} of PSC without NPs were 2.50% and 11.82

mA/cm^2 . Durian-shaped Au@Ag NPs were synthesized by changing the ascorbic acid (from 30 to 45 µl) to obtain different sizes. The proposed shape of Au@Ag NPs showed an effect of small radii of the spike ends of the durian-shaped NPs on the performance of PSCs. The results revealed that the Jsc and PCE of up to 17 mA/cm^2 and 3.73%, respectively, which implies a 44.4% improvement in short-circuit photocurrent density and 49% enhancement of the PCE compared to the reference cell (without NPs). Besides, different volume ratios of PEDOT:PSS-to-Au@Ag NPs (8%, 10%, 12%, 14%, and 16%) were prepared to optimize synthesis conditions for increased efficiency. As a result, the device with a volume ratio of 14% (PEDOT:PSS–to–Au@Ag NPs) exhibited better light absorption in a broad wavelength range from 350 nm to 750 nm, where the PCE was improved from 2.50 to 4.15%, which is a 66% increase compared to the device without NPs. In addition, durian-shaped Au@Ag NPs embedded into both the active and buffer layers were investigated. It is observed that the plasmonic device with the structure of ITO/PEDOT:PSS+Au@Ag NPs (14%)/PTB7:$PC_{71}BM$+Au@Ag NPs (4%)/Al worked better than others. Therefore, the best efficiency obtained in this research was 4.24%, which represents a 69.6% enhancement of the PCE compared to the reference cell.

CHAPTER 1

INTRODUCTION

1.1 Introduction

Solar cells serve a crucial role in energy generation and constitute a vital source of renewable energy that allows conversion of solar energy (from sunlight) to electrical energy. Solar energy is eco-friendly as it produces no pollutants. The projected decline in petroleum reserves coupled with recent upheavals in major oil-producing countries, political and financial, has clearly confirmed the need for an economical, extensive, and 'eco-friendly' energy technology. So far, solar energy conversion to photovoltaic energy has proven to be the most effective option for a long-term sustainable energy generation. Over the years, several research collaborations have been conducted to manufacture highly efficient solar cells from mostly inorganic materials such as silicon. Presently, solar cells based on silicon-wafers account for 95% of the photovoltaic cell industry, which can be attributed to the development of silicon-based semiconductor technology and enhanced single-junction efficiency power conversion (PCE) exceeding 26% (Gielen et al., 2019; Woodhouse et al., 2019). Nonetheless, polymer solar cells (PSCs) have garnered researchers and solar cell industry's interest because of their light weight, mechanical flexibility, ease of fabrication, and low cost, which allows them to efficiently power the next generation outdoor and indoor IoT (Internet of Things) devices or sensors. The conversion of light absorption into free-charge carriers is the key disparity between conventional inorganic devices and polymer-based solar cells. For example, the absorption of light in conventional inorganic materials results in the generation of free electrons and holes. Contrarily, polymer materials produce electrons-holes pairs that are referred to as excitons. Thus, the generation, transport, and accretion of charges differ between polymer and inorganic solar cells.

The fundamental principle of photocurrent generation inside PSCs is based on these key steps: light absorption and excitons generation; excitons separation to e-h pairs, and charge transport. (Chochos and Choulis, 2011; Facchetti, 2013; Marinova et al., 2017; Mazzio and Luscombe, 2014). The direct conversion of incident light on PSCs into electricity requires an active layer composed of two photoactive materials to enable optical absorption and production of excitons. The active and buffer layers are inserted between the anode and cathode that accumulate the free charge carriers as illustrated in Figure 1.1. The transparency of indium tin oxide (ITO) and poly(3,4-48 ethyl enedioxythiophene): poly (styrenesulfonate) (PEDOT:PSS) allows the transmission of the incident light in the active layer that consists of [4,8-bis[(2-ethylhexyl)oxy] benzo [1,2-b:4,5-b'] dithiophene-2,6-diyl] [3-fluoro-2-[(2-ethylhexyl) carbonyl]thieno[3,4-b] thiophenediyl (PTB7), and [6,6]-Phenyl C_{71} butyric acid methyl ester, mixture of isomers ($PC_{71}BM$). The absorption of incident light at PTB7 (donor) initiates the generation of excitons which can diffuse into the $PC_{71}BM$ (acceptor) layer. The dissociation of excitons arises when the duration of diffusing no exceeds the decomposition time. Generally, the lifetime of an exciton is about several nanoseconds. The diffusion length of the exciton in polymer/organic materials varies between 1 and 10 nm, which critically constrains the thickness of the absorbing layer (Rafique et al., 2018).

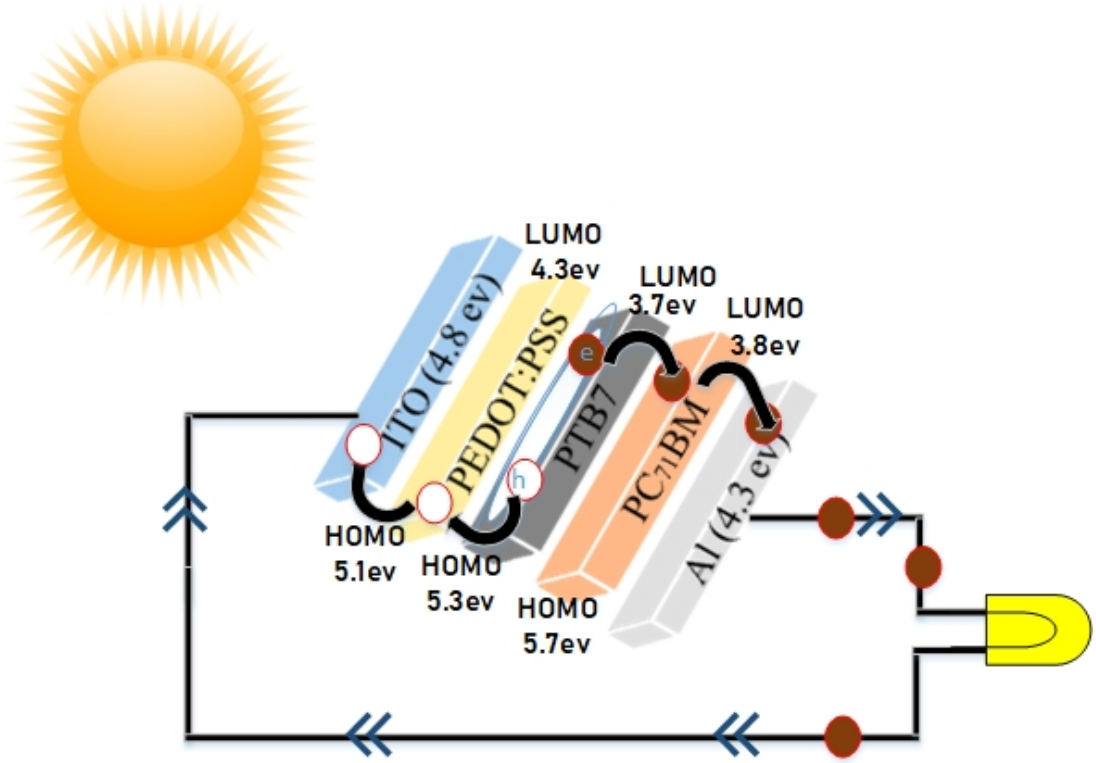

Figure 1.1: Schematic structure of working of PSCs. The device consists of: ITO/ buffer layer (PEDOT:PPSS)/ active layer (PTB7:$PC_{71}BM$)/ Al.

In particular, the performance of any solar cell depends on the cell's capacity to absorb incident light, and the exciton dissociation's effectiveness, and the accumulation of charge carrier. However, a major constraint that limits the performance of PSCs is the inherent trade-off between effective absorption of light and accretion of photogenerated excitons. In other words, the PSCs are constrained by low PCE and open-circuit voltage (V_{oc}) due to their inadequate light absorption, low charges diffusion length, and high recombination rate leading to exciton quenching in the active layer (Shin et al., 2019; Tong et al., 2020). Therefore, the PCE of PSCs is still around 17% (Zhan et al., 2020; Zhu et al., 2020), which is less than their inorganic counterparts. However, this new generation of solar cells is considered a potential substitute power source for future smart electronic devices (Green et al., 2006; Kwon et al., 2012; Xu et al., 2014).

To achieve efficient absorption of photons in bulk heterojunction (BHJ) PSCs, there must be effective mechanisms to exploit the maximum amount of light falling

on the PSCs. Although, the limited absorption of the incident light can be enhanced by a thicker active layer, this leads to the recombination of excitons, resulting in lower efficiency (Shen et al., 2014; Yuan et al., 2016; Zhao et al., 2016). Thus, a variety of harnessing energy techniques are developed to enhance the photoactive layer's absorption. As such, PSCs have been modified or functionalized to boost the capacity of the thin active layer to absorb light by means of periodic grating structures in electrodes, controlling the morphology of the layers, reconfiguring optical device structure for light distribution, and incorporating metallic nanoparticles (MNPs). Among these strategies, MNPs have gained a greater interest as an efficient approach for trapping light in the photoactive layer and improving the dissociation of excitons because of their near-field coupling effect (Agrawal et al., 2018; Atwater and Polman, 2011; Chen and Ming, 2012; Feng et al., 2018; Mola et al., 2021; Putnin et al., 2019; Xue et al., 2011).

The incorporation of MNPs into the buffer layer (i.e., PEDOT:PSS) takes advantage of the electrical hole collection enhancement, far-field scattering effect, and localized surface plasmon resonance (LSPR) by initiating chemical and morphological changes in the buffer layer. Exciton quenching can also be avoided by identifying the sites of MNPs at the indium tin oxide (ITO) or at the buffer layer, or between the active and buffer layers. The effect of incorporating MNPs of gold (Au) and silver (Ag) on the performance of PSCs was investigated because of the relatively high scattering strength, chemical stability, and remarkable LSPR optical properties. Several metal nanostructures have been functionalized to significantly augment the enhancement of light absorption, such as the composite NPs with different metals (Choy, 2014; Lu et al., 2013; Stratakis and Kymakis, 2013), Au nanospherical (Said et al., 2019) and nanorods (Gao et al., 2018), Au nanostars (Ren et al., 2016), Ag with multiple-shapes (Hao et al., 2017), truncated octahedral (Wang et al., 2011b), decahedral/icosahedron Ag NPs (Chen et al., 2018), mixing of the Au and Ag NPs (Gao et al., 2017), Au NPs with graphene shell (Au NPs@Gr) (Rezaei et al., 2019), and Au@Ag nanocube (NC) (Baek et al., 2014). Therefore, the performance of PSCs embedded with MNPs

strongly depends on the size, shape, and volume ratios of MNPs into the hole transport layer (HTL) or active layer.

1.2 Problem statement

PSCs suffer from insufficient incident light absorption, which makes the PCE lower than their inorganic counterparts. A broad spectrum of LSPR is needed to boost a significant amount of light absorption improvement. Au and Ag are distinctive as their free electron densities are within a precise range that allows the LSPR peaks of nanoparticles to be discernible from the visible spectrum (Xia and Halas, 2005). In addition, it applies a dominant photon scattering efficiency that expands the length of the photon path within the cell. Several studies that evaluated the PCE of PSCs reported marked improvement by embedding Ag or Au NPs in the photovoltaic layers at different positions of PSCs (Ali et al., 2020; Babaei et al., 2020; He et al., 2015a; Koul et al., 2020; Nair et al., 2020; Sun et al., 2020; Xu et al., 2020). Nonetheless, the scattering efficiency of Au NPs is relatively lesser compared to its level of self-absorption. On the contrary, the scattering efficiency of Ag NPs is comparably high, although the LSPR region is restricted to a wavelength range of 400–500 nm. Thus, maintaining the broad wavelength range, especially at long wavelengths, is a complex process.

To overcome this problem, researchers were focused on the mixing of Au and Ag NPs together into PSCs (Gao et al., 2017; Xu and Hou, 2018; Xu et al., 2014). However, Au and Ag NPs present an intense enhancement of the electric field at low and high energies only, which is a dilemma that is encountered when using mixtures of Au and Ag NPs. In addition, the absorption, scattering of the incident light, and LSPR effect of the NPs are strongly dependent on their shapes, sizes, and volume ratios. Therefore, in order to enhance both scattering efficiency and broad LSPR region especially at the long-wavelength range, it is important to develop MNPs structures. In this study, a new type of plasmonic cores is proposed to improve the

PCE of PSC. Durian-shaped Au@Ag NPs (with many sharp spikes) were prepared in order to examine the effect of the small radii of the ends of spikes on performance PSCs. This is imperative as the plasmonic effect of sharp spikes in PSCs is yet to be investigated. Furthermore, in this study, the plasmonic effect of durian-shaped Au@Ag NPs in both the active and buffer layers was investigated to demonstrate the combinatorial impact of the high scattering power of Ag NPs and the broad spectral response of Au NPs. This will improve the LSPR effects and increase light absorption in the active layer.

1.3 Objectives of study

1. To synthesise, characterized and optimized durian-shaped Au@Ag NPs with different sizes embedded in PSCs.

2. To investigate the effects of different volume ratios of durian-shaped Au@Ag NPs in the buffer layer.

3. To examine the relationship on the effects of durian-shaped Au@Ag NPs related to its locations in PSCs (PEDOT:PSS and PTB7:$PC_{71}BM$) layers.

1.4 Scope of study

This study's scope is confined to synthesising durian shape Au@Ag core-shell NPs, and embedding them into PSCs to enhance the PCE compared to the reference cell (without durian-shaped Au@Ag NPs). Au NPs as a core and Ag NPs as a shell around Au NPs' surface were chosen due to their relatively high scattering strength, chemical stability, and remarkable LSPR optical properties. The type of polymer solar cell was identified among other types because of its light weight, mechanical flexibility, ease of fabrication, and low cost. The proposed Au@Ag NPs confirmed the effect of small radii of the spike ends of the durian-shaped on the electric parameters of PSCs.

1.5 Contribution of the thesis

This study contributes to improving the performance of polymeric solar cells through plasmonic NPs effects as follows:

1. Proposing a new shape of NPs (durian-shaped Au@Ag NPs) with different sizes and embedding it into PSCs.
2. Determining the appropriate amount of NPs in the buffer layer (PEDOT:PSS).
3. Demonstrating the dual effect with suitable volume ratios of NPs embedding into each of the PTB7:$PC_{71}BM$ and PEDOT:PSS.

1.6 Thesis outline

This thesis comprises five chapters. beginning with introduction, problem statement , objectives, contribution, and scope of the study. Chapter Two provides a theoretical background, working principle of the PSCs, plasmonic NPs effects, and previous works of PSCs embedded with plasmonic NPs. Chapter Three is dedicated to identifying the materials used in this research, synthesis of Au@Ag durian-shaped NPs, explaining PSCs fabrication and characterization. Results and discussion of this work are displayed in Chapter Four. Finally, in Chapter Five, this thesis ends up with the conclusions and future works to enhance the efficiency of the PSCs.

CHAPTER 2

THEORETICAL BACKGROUND AND LITERATURE REVIEW

2.1 Introduction

This chapter started by describing the types, theoretical background, and fundamental properties of solar cells. In addition, it focuses on the working principles, materials, and advantages of PSCs. Next, it describes the plasmonic effect of NPs and the electromagnetic fields of nanoparticles with spiked surfaces. The performance of PSCs embedded with NPs based on the literature review was listed out in the last section of this chapter.

2.2 Solar cells generations

Solar cells are divided into three generations. First generation solar cells are costly to manufacture, and they have good stability. The second generation solar cells are fabricated of thin films, resulting in a lower cost per Watt compared to the first generation. Third generation cells have good efficiency despite their instability compared to the first generation. To this end, many researchers are working to develop inexpensive third generation solar cells. For more details, the solar cell types are divided according to the generation of each as follows:

2.2.1 First generation

Due to its high efficiency and stability, first generation silicon technology now dominates the global photovoltaic industry, accounting for more than 90% of solar cells fabricated. This generation includes single-crystal and multi-crystal solar cells, and these are the oldest used technology types. Figure 2.1 shows the examples of the first generation solar cells. Solar cells of the first generation are fabricated using wafers. Each wafer is capable of delivering between 4-5 Watt of electricity. Solar

modules, which are made up of 60 cells, are used to increase the output of electricity. The two kinds of first generation solar cells are distinguished by their crystallisation levels. If the whole wafer is composed of just one crystal, it is referred to as a single-crystal solar cell. If the wafer contains crystal grains, the solar cell is referred to as a multicrystal solar cell. Although single-crystal solar cells have greater efficiency than multicrystal solar cells, multicrystal wafer manufacturing is simpler and less expensive (Green, 2013; Ibrahim, 2011; Khatibi et al., 2019; Sharma et al., 2015; Yerokhov et al., 2002).

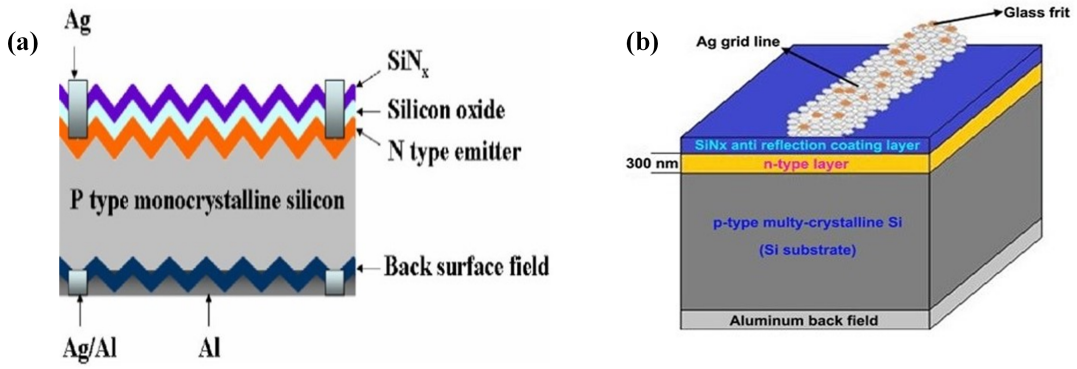

Figure 2.1: Schematic of the first generation of solar cells; (a) single-crystal solar cells (Liu et al., 2014) and (b) multi-crystal solar cells (Wang et al., 2017).

Silicon solar cell technologies have progressed quickly and are now commercially significant. However, the primary drawback is the high cost of fabrication. The silicon solar cell fabrication process entails the following steps: electrical reduction of quartz sand, crystal growth from the liquid silicon, melting of the polysilicon, cutting and polishing to a silicon wafer, and assembly into a solar cell. Besides, the reduction process needs a high current density and a temperature of over 1000°C. High temperatures are also required for the melting and crystal formation processes. This process uses a lot of energy and leads to the high cost of silicon wafers. Furthermore, crystalline silicon's bandgap is about 1.1 eV, which is not an ideal value for PV applications. As a consequence, basic silicon's absorption edge is located in the infrared wavelength range, and a significant part of the photon energy with shorter

wavelengths is lost. In addition, silicon's absorption coefficient is low, requiring silicon wafers to be thicker than 100 μm to provide adequate light absorption unless light trapping methods are used (Chopra et al., 2004). Increasing the thickness requires more materials, which means increasing the cost of fabrication.

2.2.2 Second generation

Researchers have developed several new inorganic solar cells with improved photoelectric properties to avoid the problems of the first generation. Majority of these solar cells' materials are two-element or multi-element such as amorphous silicon (Qarony et al., 2017; Sai et al., 2018), copper indium gallium selenide (CIGS) (Mohan and Paulose, 2019; Rezaei et al., 2020), cadmium telluride (CdTe) (Devendra et al., 2021; Kapadnis et al., 2020), and gallium arsenide (GaAs) (Kumar et al., 2020; Papež et al., 2021) as shown in Figure 2.2. The energy levels of these materials are carefully regulated to get an optimal performance for solar cells and their bandgaps. Because their absorption coefficients are typically high, the active layer of the second generation solar cells may be as thin as a few hundred nanometers. Thin-film technology is a fabrication method for several of these materials and it differs from more conventional methods. The film manufacturing method for a CIGS solar cell, for example, is typically vacuum-based: first, copper, gallium, and indium are co-evaporated onto a substrate, and then anneal the resultant film using selenide vapour. The thickness and the depositing conditions of the film have a significant influence on the physical, chemical, and electrical characteristics of the film, allowing for precise device performance.

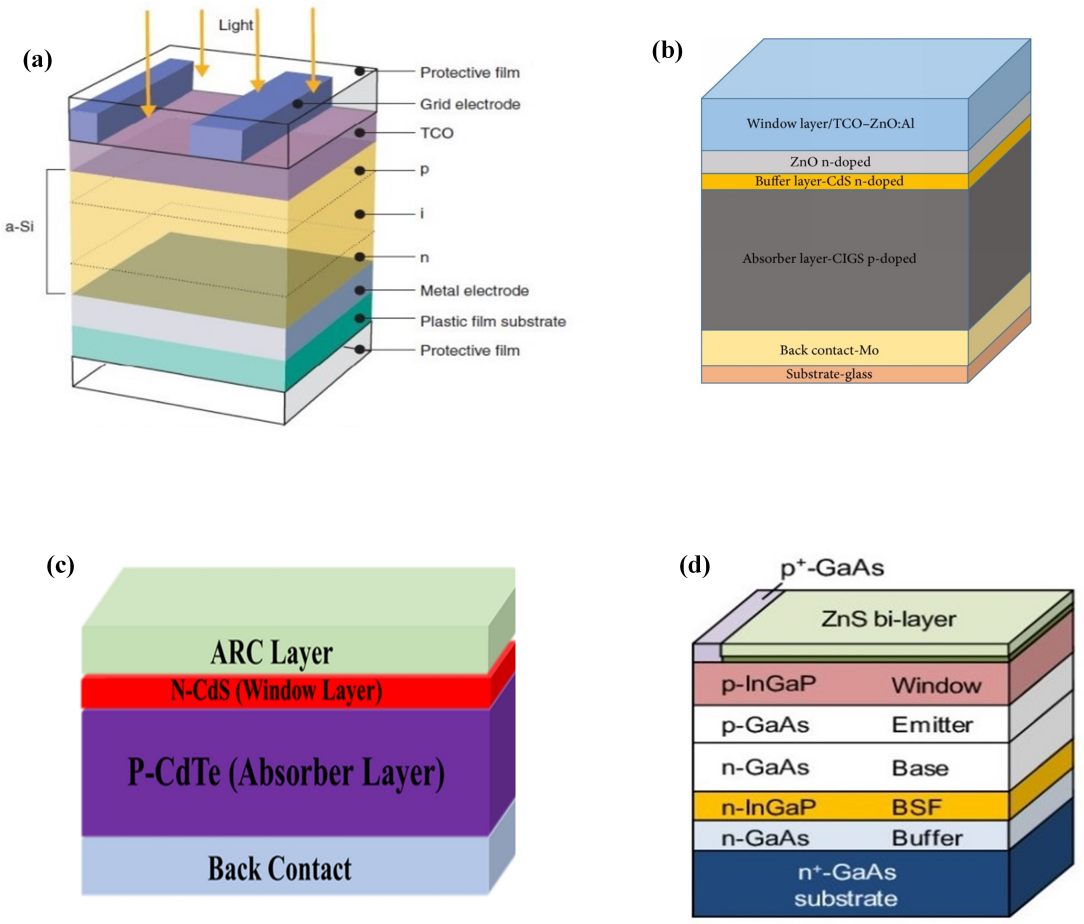

Figure 2.2: Schematic of the second generation solar cells; (a) amorphous silicon solar cells (Fraas, 2014), (b) copper indium gallium selenide (CIGS) solar cells (Parisi et al., 2015), (c) cadmium telluride (CdTe) solar cells (Devendra et al., 2021), and (d) gallium arsenide (GaAs) solar cells (Leem et al., 2013).

Furthermore, the PCE and the fabrication cost are the two most significant variables that affect the energy payback period. Because the active layers of the thin-film solar cells may be considerably thinner than in conventional solar cells, the use of raw materials is significantly decreased, as is the cost. Because this generation of solar cells came out later than conventional silicon solar cells, certain issues like stability and toxicity remain unresolved, thus it may take longer for them to catch up in market share.

2.2.3 Third generation

Third generation solar cells based in high-efficiency thin films, which are made from nanostructured materials, have detained a lot of interests because of their simple production process, availability of materials, and cheap cost. This prompted researchers to work on producing highly efficient and more stable solar cells at the lowest cost. Dye-sensitized solar cells (DSSCs) (Andualem and Demiss, 2018; Gong et al., 2017), organic solar cells (polymer devices) (Berger and Kim, 2018; Gurney et al., 2019; Hou et al., 2019), quantum dot-sensitized solar cells (QDSSCs) (Bhambhani, 2018; Mora-Seró, 2020; Sahu et al., 2020), perovskites solar cells (Mahapatra et al., 2020; Siavash Moakhar et al., 2020; Yang and You, 2017), and multi-layer tandem devices using amorphous silicon (Jošt et al., 2020) are all examples of third generation solar cells as shown in Figure 2.3. The newly studied polymer and perovskite materials, which have emerged as a viable alternative owing to their cost effectiveness and high efficiency, are one of the important types of solar cells, because of their lightweight, mechanical flexibility, ease of fabrication, and low cost, which allows them to efficiently power the next generation outdoor and indoor IoT devices (Kim et al., 2020; Li et al., 2018; Singh et al., 2019; Xie et al., 2021).

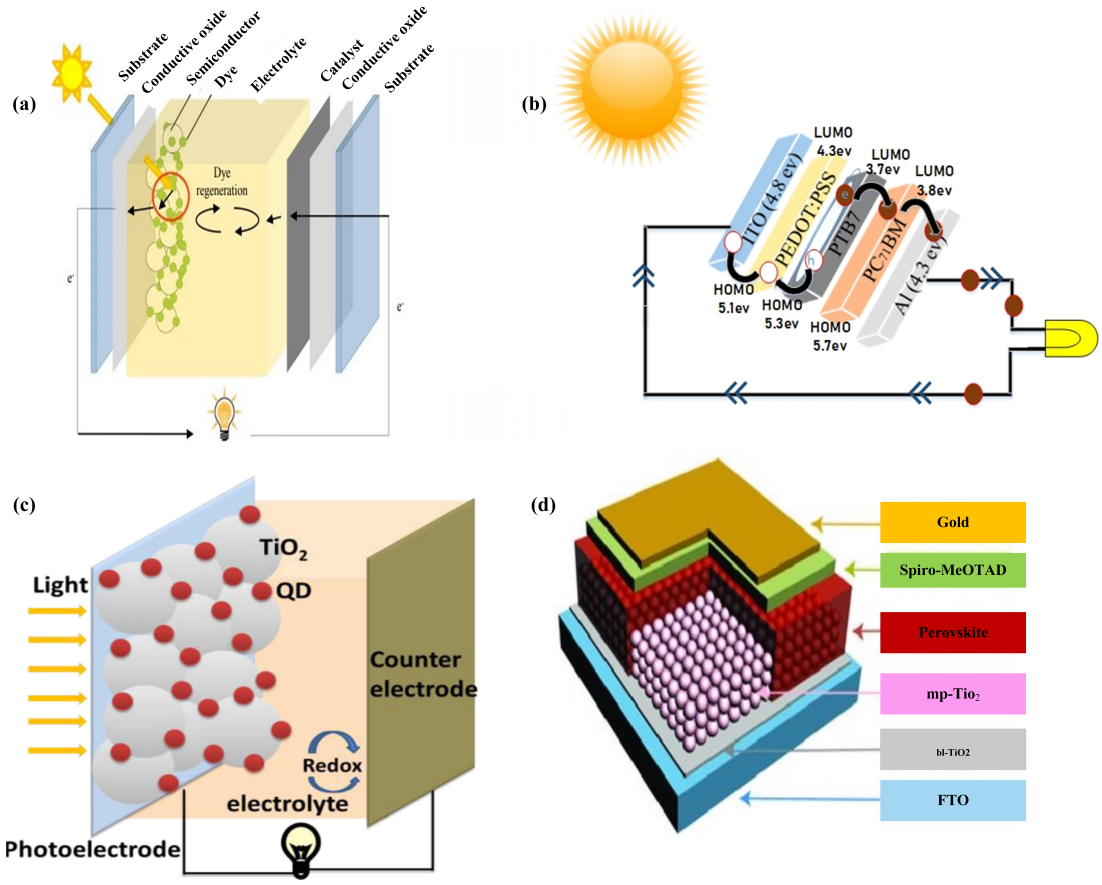

Figure 2.3: Schematic of the third generation solar cells; (a) DSSCs (Parisi et al., 2014), (b) PSCs, (c) QDSSCs (Tian and Cao, 2013), and (d) perovskite solar cells (Vivo et al., 2017).

On the other hand, there are four basic kinds of semiconductor junction architecture that may be used to convert solar energy into electricity (Yu and Heeger, 1995). The following are examples of these types:

1. Homojunctions: are made up of the p-n junctions of a single semiconductor material that is doped with impurities. Homojunctions, like the typical p-n junction silicon solar cell, has a high junction efficiency.

2. Heterojunctions: are a p-n junction comprising two various semiconductors, one with a wide bandgap that serves as a window for the junction and the other with a small bandgap that absorbs solar radiation.

3. Metal-insulator-semiconductor junctions: this structure exhibits the charges separation characteristics of Schottky junctions while avoiding direct metal-semiconductor contact. This kind of solar cell has additional layers (conductor, oxide, and semiconductor).

4. Semiconductor-Insulator-Semiconductor (SIS) junctions: the SIS device is composed of a lower semiconductor layer, an upper semiconductor layer, and a central buffer layer placed between the lower and higher semiconductor layers.

2.3 Advantages of polymer solar cells

Polymer materials have interested the scientific community due to their unique properties. Conjugated polymers have alternating C-C single bonds and C=C double bonds, including carbon, hydrogen, and additional heteroatoms such as nitrogen, oxygen, and sulfur. In general, they are insulators that become semiconductors when they produce charged particles (either holes or electrons) with electrodes or chemicals. When charges are injected into a conjugated system, the charges may delocalize and produce current in an electric field. Organic/polymer semiconductor materials are thought to be potential substitutes for inorganic absorbers. The primary reason is that PSCs are much less expensive than inorganic solar cells. In addition, the whole synthesis, purification, and manufacturing process may be done at a low temperature with little energy usage.

Thermal evaporation deposition is the more common process for thin-film fabrication. The solution-processing technique is a thin-film technology that uses a polymer solution containing material as electronic ink to be printed on the substrate's surface. The light absorbing layer (active layer) in PSCs is typically in the thickness range of 100-200 nm due to the high absorption properties of the polymer materials. Because of the thinness of the layer, only a few milligrams of the ingredients are needed to cover the surface area of the substrate, which can be several hundred square centimeters. The solution process technique is advantageous not only in terms of

cheap material costs, but also in terms of high throughput and large-area production of polymer solar cells using small amounts of polymer materials. Polymer materials may also be produced on flexible substrates to create flexible and light-weighted electrical devices owing to their unique properties. In conclusion, the advantages of PSCs outlined below: (Scharber and Sariciftci, 2013)

1. Semitransparent
2. Production costs are much cheaper compared to inorganic solar cells
3. Wider market opportunities, such as IoT applications
4. Easy integration into other products
5. Flexibility and low-weight of the solar cells module
6. Short energy payback period and minimal environmental effect

2.4 Working principle of polymer solar cells

The significant disparity that differentiates the established inorganic devices and PSCs is the conversion route of light absorption into free charge carriers. More specifically, the process of light absorption in conventional inorganic materials results in the generation of free electrons and holes, whereas that of PSCs leads to the creation of bound electron-hole pairs referred to as excitons. Therefore, the generation, transport, and accumulation of charges are different for polymer-based SCs and their inorganic counterparts (Figure 2.4). The essential mechanism of photocurrent generation inside PSCs entails four key steps (Chochos and Choulis, 2011; Dou et al., 2013; Facchetti, 2013): light absorption and production of exciton, exciton diffusion, partition of charges, and transport and collection/accumulation of charges. The direct conversion of the incident light on polymer solar cells into electrical energy requires an active layer that comprises two active materials (i.e., PTB7 and $PC_{71}BM$) to allow the optical absorption and creation of excitons. The

active and buffer layers are inserted between two metallic electrodes (anode and cathode) that accumulate the free charge carriers. One of the electrodes is made transparent to allow the transmission of the incident light within the solar cell (Marinova et al., 2017).

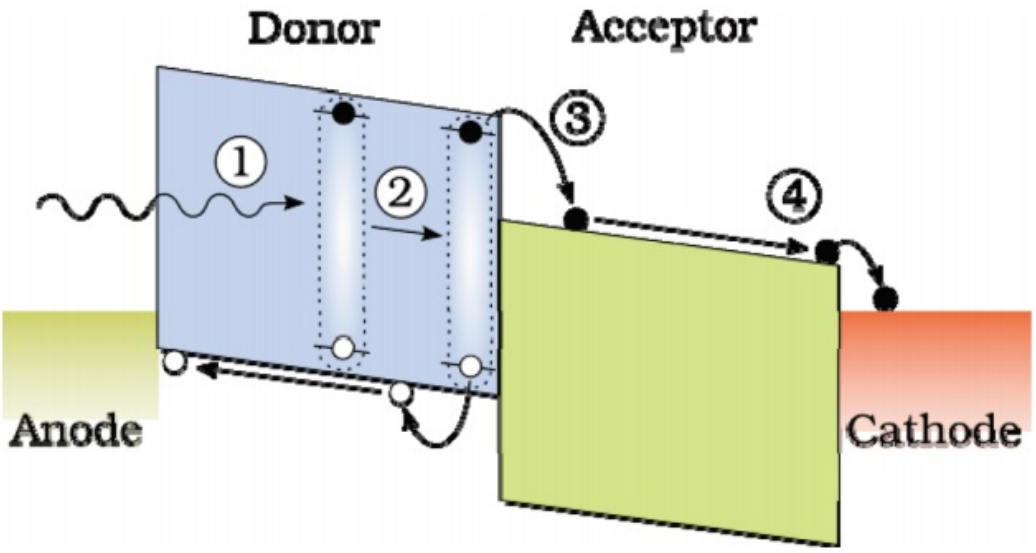

Figure 2.4: A two-dimensional energy diagram of PSCs representing the four main steps to generate photocurrent (Heremans et al., 2009).

2.4.1 Light absorption and generation of excitons

PSCs are composed of electron charge-transport layers and an photoactive layer. The photoactive layer, which is composed of a combination of p-type and n-type materials, has a dual function. It enables the separation of charges, and plays the role of an optical harvester. The loss of optical-light induced by reflections at the interface between air and substrate needs to be drastically reduced to enhance the intensity of light transmission into the active layer. Hence, the first material to absorb the incident light in the device structure should be as transparent as possible. The effectiveness of light absorption is dependent on the absorption coefficient (α). Organic materials usually possess a higher absorption coefficient than inorganic/crystalline or multi-crystalline silicon, therefore they exhibit efficient optical processing with a thin layer at a particular wavelength (i.e., 100–200 nm) (Brédas et al., 2009). In contrast,

polymer materials are generally characterized by narrow absorption spectra with no optical absorption in the spectrum's red and near-infrared regions (Figure 2.5). Hence, the absorption of light inside the active layer generates electrically neutral excitons. Thus, it is imperative to modify the bandgap and broaden the absorption region, which many researchers currently undertake.

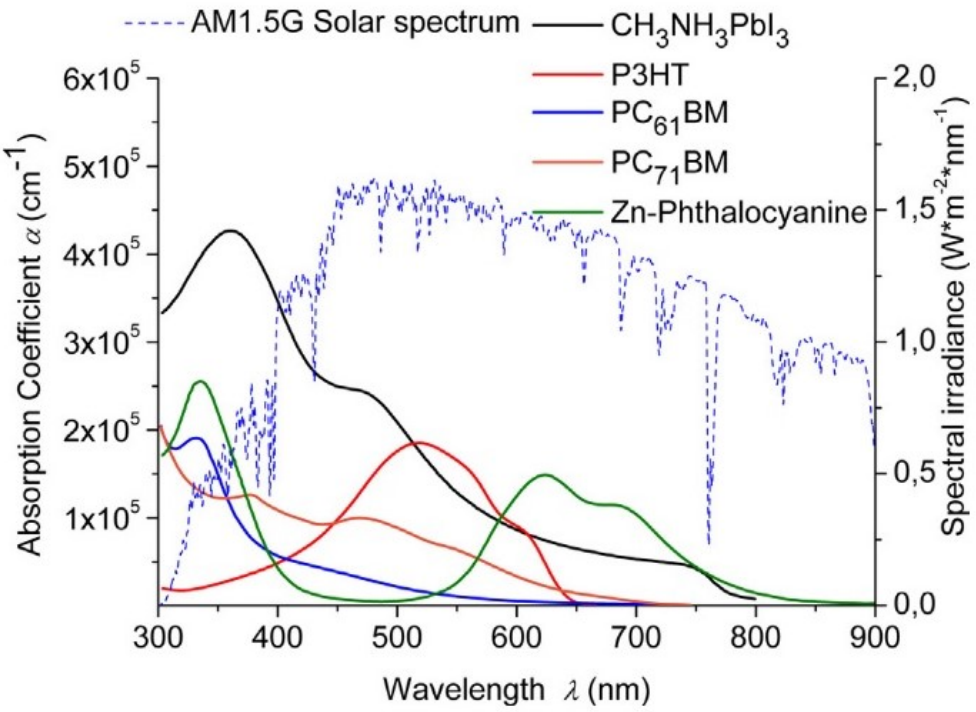

Figure 2.5: Absorption coefficient versus wavelength of thin films ($CH_3NH_3PbI_3$, P3HT, $PC_{61}BM$, $PC_{71}BM$, and Zn-phthalocyanine) with the AM 1.5G solar spectrum (Marinova et al., 2017).

2.4.2 Diffusion of excitons

Ideally, the generation of excitons results in creating free electrons and holes when a molecule absorbs light. However, this phenomenon is dependent on the migration of excitons towards the acceptor/donor interface (Feron et al., 2012). Exciton diffusion efficiency is controlled by layer thickness and length of diffusion (L_D), as expressed in Equation 2.1, where L_D denotes the distance that an exciton traverses throughout its lifetime, (τ) symbolizes the lifetime of the exciton, and (D) is defined as the diffusion coefficient. Due to the mechanisms of radiative and

non-radiative decay confine exciton transport, the lifetime of an exciton is determined to be about several nanoseconds while the exciton diffusion length in organic materials is approximately 5-20 nm (Sauvé and Fernando, 2015). Therefore, any increase in the charge separation probability requires the generation of all excitons within the donor/acceptor interface.

$$L_D = \sqrt{D\tau} \tag{2.1}$$

2.4.3 Exciton dissociation

The binding energy of excitons is relatively large (i.e. 0.3 to 1 eV) (Sauvé and Fernando, 2015). Thus, the conversion of excitons to free charge carriers requires the subduing of electrostatic binding energy by the electron-hole pairs, with external and internal electric fields contributing to this phenomenon. A highly intense and discrete EM field generated at the interfaces, as a result of which radical transformation of the potential energy occurs. There are two types of free charge carrier losses that may occur if the produced EM field is insufficient to allow separation beyond electrostatic attraction, namely geminate and non-geminate recombinations (Mazzio and Luscombe, 2014; Sariciftci and Sun, 2005).

2.4.4 Charge transport and collection

As the exciton arrives at the donor/acceptor interface, it is detached into electron-hole pairs that are mobilized towards the electrodes to generate the photocurrent. The transport of charges is efficient if the driving force is sufficiently strong to thrust the electrodes' free electrons and holes. The disparity between the highest occupied molecular orbital (HOMO) of the donor and the lowest unoccupied molecular orbital (LUMO) of the acceptor produces a slope at the donor-acceptor interface. Along with the maximum value of V_{oc}, the transportation of charge carriers towards the electrodes is dependent on the internal electric field as shown in Figure

2.6 (Marinova et al., 2017; Rafique et al., 2018). Finally, the electric charges are collected by the electrodes (anode and cathode).

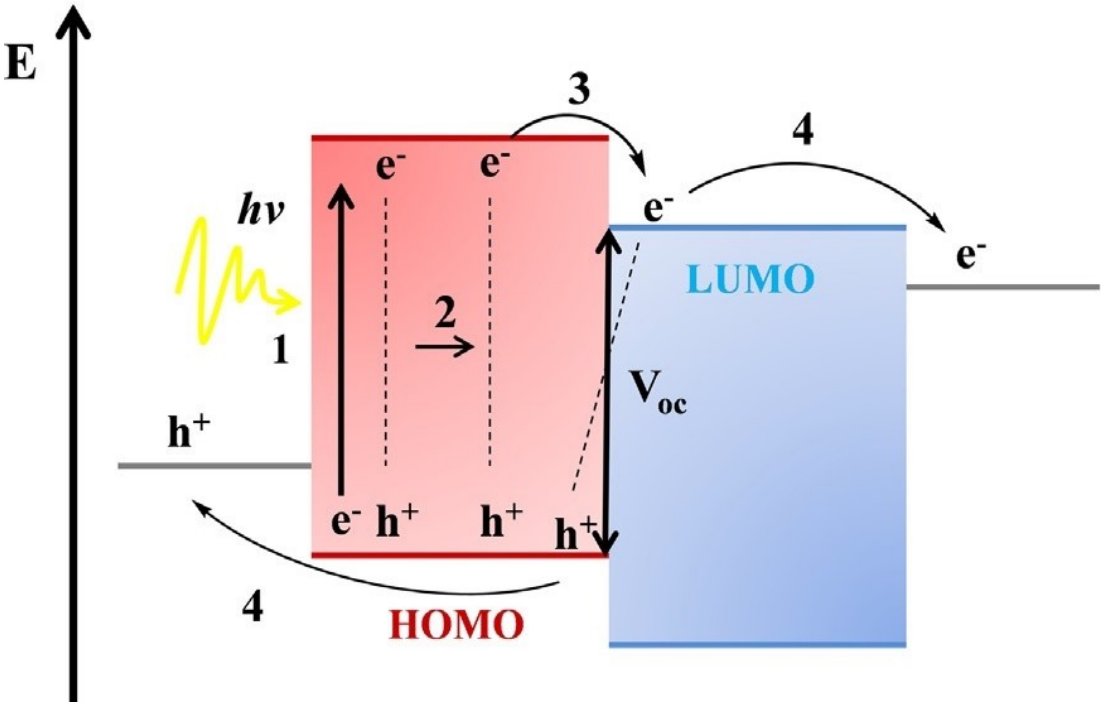

Figure 2.6: Band diagram and main processes in PSCs (Marinova et al., 2017).

2.5 High-performance materials in polymer solar cells

2.5.1 Donor materials

The donor material donates electrons and transports holes by absorbing incident photons. The development of donor polymer materials is an important step in developing the performance of PSCs. Figure 2.7 shows the molecular structure of some donor polymer materials that exhibited the best PSCs' performances nowadays. These polymers are Poly[1,2-b:4,b]dithiophene,6-diyl]4,bis-(2-ethyl-hexyl-thiophene-yl)[3,4-b]-4,6-diyl]-benzo-alt-[2-(ethyl-hexanoyl)-thieno (PBDTTT-C-T), poly (3-hexylthiophene) (P3HT), PTB7, and PBDB-T. These polymers exhibit high absorption, high hole mobility, a sufficient absorption range and energy levels, good solubility, and good morphology, which are all necessary conditions for increasing PSCs' efficiency. In particular, PTB7 is one of the most promising donor polymer

materials owing to its short-branched side chains, which provide the polymer with excellent solubility for the fabrication of solar cells. Moreover, PTB7 shows a strong absorption from 550 nm to 750 nm and a narrower optical bandgap (about 1.6 eV) (Barreiro-Argüelles et al., 2018; Chander et al., 2018; Ghazy et al., 2020; Liu et al., 2018b; Lu and Yu, 2014; Xue et al., 2018).

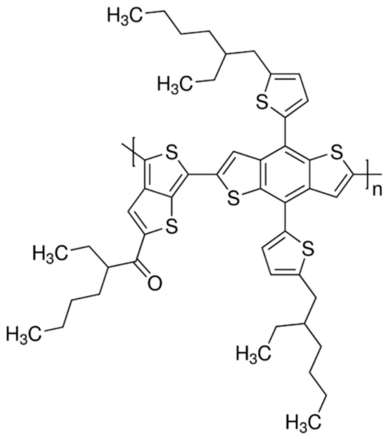

PBDTTT-C-T

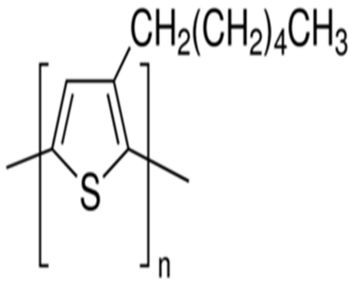

P3HT

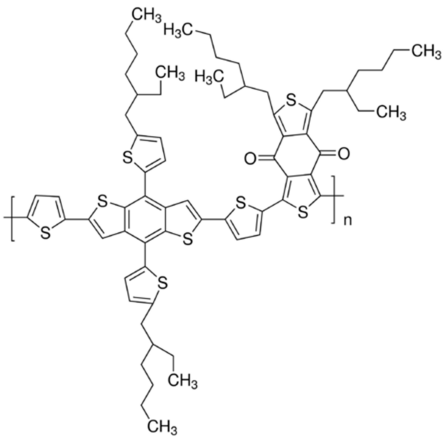

PBDB-T

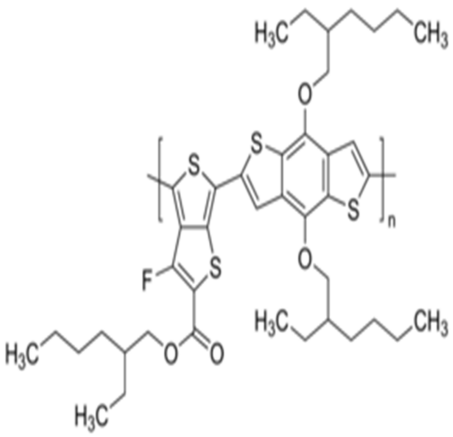

PTB7

Figure 2.7: The molecular structure of some donor polymer materials (Kim and Lim, 2014; Zhang et al., 2018).

2.5.2 Acceptor materials

The polymer acceptors are based on some electron-deficient moieties (n-type polymer acceptors) that lower the HOMO and LUMO energy levels of the polymer. Cyano (N-C) substitution, benzothiadiazole (BT), perylene diimide (PDI), naphthalene diimide (NDI) are the four most common groups of polymers' acceptors (Kim and Lim, 2014). Some of the molecular structures are illustrated in Figure 2.8.

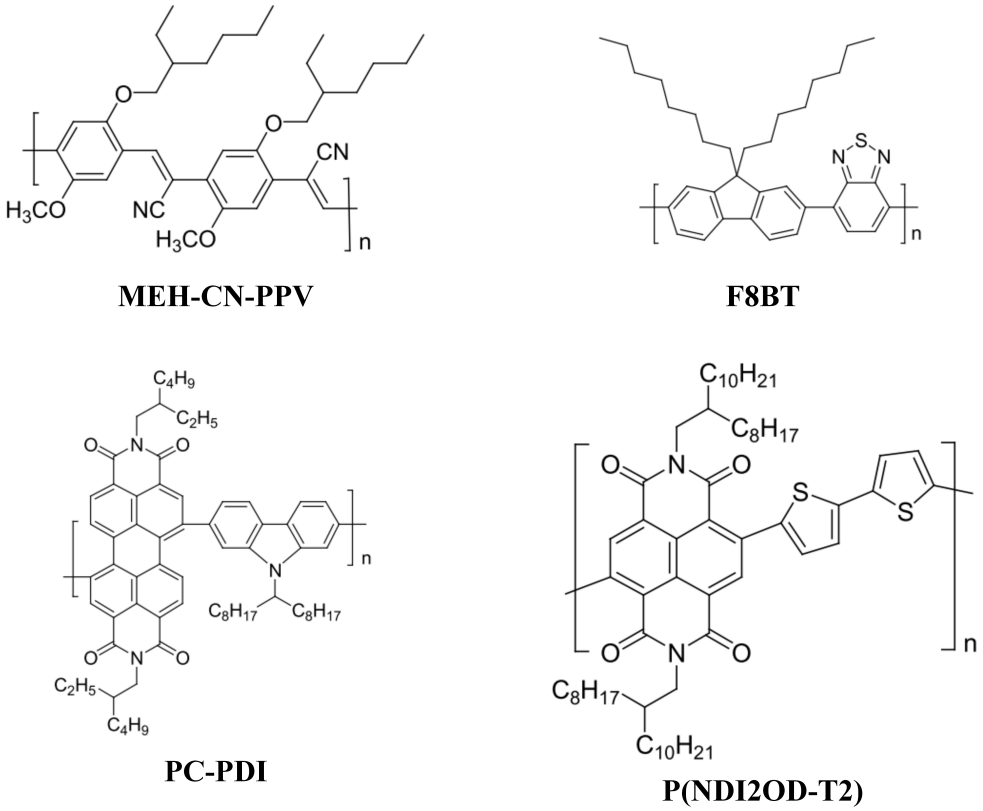

Figure 2.8: The molecular structure of some acceptor polymer materials (Kim and Lim, 2014).

However, polymer acceptor-based blend films have challenging morphological control, particularly in polymer-polymer systems. This phenomenon is caused by the high degree of miscibility that exists across various polymers. Once deposited on the substrate, the polymers often exhibit little selectivity during the aggregation process, resulting in relatively impure domains. Due to the impure domains, mobility will be reduced and charge recombination will be increased. This is one of the primary

reasons why polymer acceptor-based solar cells have such poor efficiency.

Fullerene, typically [6,6]-phenyl-C61-butyric acid methyl ester ($PC_{61}BM$) and [6,6]-phenyl-C71-butyric acid methyl ester ($PC_{71}BM$) as shown in Figure 2.9, are the most commonly used in PSCs, because of their high electron affinity, mobility, and high charge transfer rate when accepting electrons from the donor polymer. The ball-shaped structure not only makes excellent contact with the polymer's pi system but also promotes miscibility and therefore a desirable blend morphology (Bernardo et al., 2020; Liao et al., 2019; Mühlbacher et al., 2006).

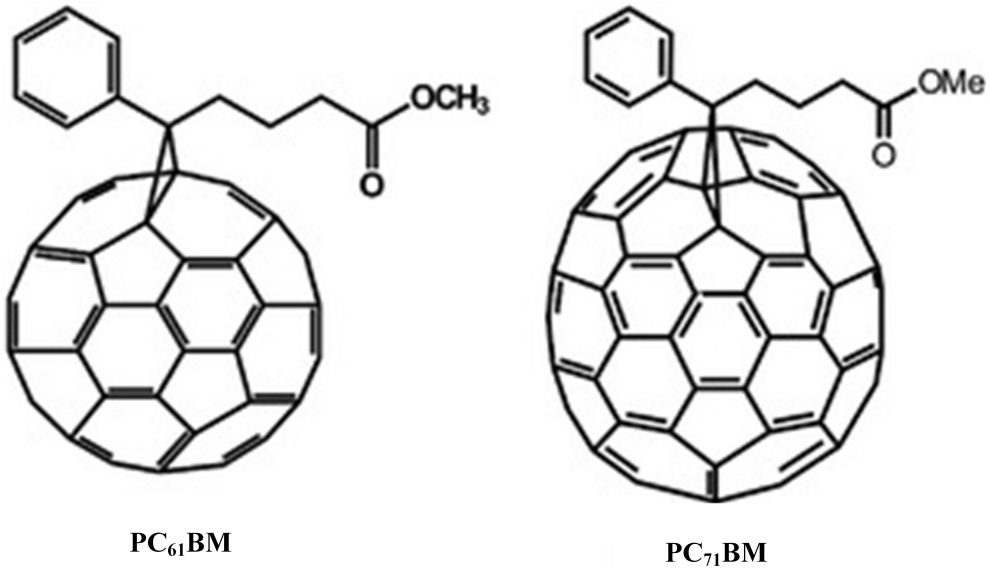

Figure 2.9: The molecular structure of $PC_{61}BM$ and $PC_{71}BM$ (Bernardo et al., 2020).

2.5.3 Bulk heterojunction

The work function of electrodes in the bi-layer system (containing separate donor and acceptor layers) gives less impact on the photovoltaic performance, primarily governed by the intrinsic characteristics of the donor and acceptor materials. Despite improvements in the efficiency of charge dissociation, the structure of the bilayer remains limited. Moreover, electrons-holes pairs must transfer to the donor-acceptor interface, and the distance between the bulk and the interface is long for excitons with

a short lifetime. Therefore, the researchers focused to develop a new structure of films to enhance solar cell performance.

To overcome this problem, Yu et al., and Hall et al., developed solution-processed bulk-heterojunction structure (BHJ) PVs (Halls et al., 1995; Yu et al., 1995). In BHJ PVs, the donor and acceptor materials are closely mixed with a 20-30 nm scale of phase separation length, which is smaller domains than in the bilayer structure, allowing more excitons to easily diffuse and dissociate. Besides, The BHJ interface area is considerably bigger than the bi-layer, resulting in substantially more exciton dissociation sites. The donor domains, as well as the acceptor domains, are still connected to one another and to the electrode. This ensures that when the excitons dissociate, electrons and holes are transported easily from the interface to the electrodes.

On the other hand, the BHJ solution's morphology is critical because the separated e-h must be collected in the electrodes. However, there is no defined orientation for the internal fields of the e-h inside the active layer. This implies that a strong pushing force should be guiding them toward the appropriate electrodes. P-type materials are designed to transport holes, whereas n-type materials are supposed to transport electrons. Therefore, the mixture should consist of a bicontinuous network. as shown in Figure 2.10 (Hoppe and Sariciftci, 2006; Li et al., 2012; Yang and Loos, 2007). The most frequently used BHJ photoactive materials were synthesised by combining PTB7:$PC_{71}BM$ due to high conductivity. Moreover, PTB7 is characterized by a strong charge carrier mobility and low bandgap.

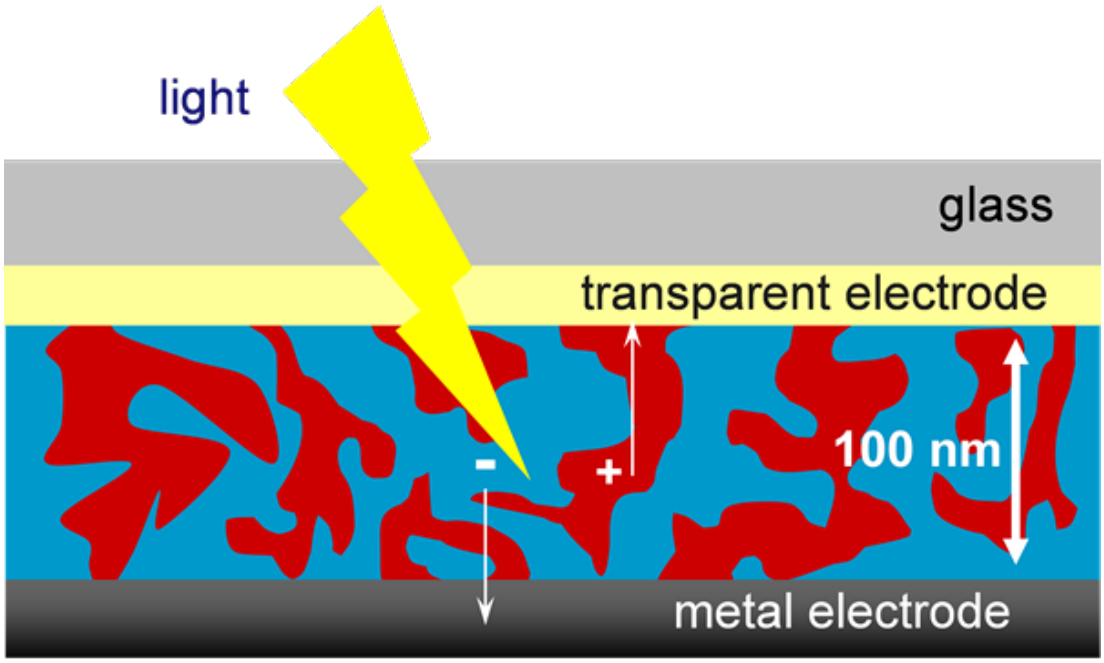

Figure 2.10: Schematic of BHJ with top and back electrodes (donor and acceptor materials were colored differently) Mehdizadeh Rad et al. (2018).

2.6 Generation and recombination mechanisms

The term "generation" refers to an electrical excitation event that increases the number of available free carriers for carrying charge. Recombination is an electronic relaxation in which the number of free carriers is reduced. Generation mechanisms necessitate the utilization of energy, which is supplied by light (photons). Recombination is an energy-release process with the opposite generating processes. There is a recombination process for every generating process. Photogeneration is the term used to describe the generation of charges in solar cells as a result of light absorption. Beginning with the absorption of the incident light and the electron is promoted from the valence band to the conduction band, the creation of an electron-hole (exciton) is the first step in this process. Besides, the decay of an electron from the conduction band to the lower state is known as recombination (Howard and Laquai, 2010; Moses et al., 2001; Zhang and Holmes, 2017).

The absorption coefficient (a) quantifies the amount of light that is attenuated as it passes through the solar cell's absorber material. When light is incident on the solar